Journal of Advanced Research in Ocean Engineering 4(1) (2018) 035-046
https://dx.doi.org/10.5574/JAROE.2018.4.1.035

Safety Analysis for Installation of Offshore Structure based on Proportional-Derivative Control Strategy with Multibody System

Ju-Hwan Cha[1], Bo-Woo Nam[2], and Sol Ha[1*]

[1]*Department of Naval Architecture and Ocean Engineering, Mokpo National University, Jeollanam-do 58554, South Korea*
[2]*Korea Research Institute of Ships & Ocean Engineering, Daejeon 34103, South Korea*

(Manuscript Received January 27 2018; Revised February 28, 2018; Accepted March 22, 2018)

Abstract

In this paper, safety analysis of the process of installing offshore structures such as manifolds and jacket-type substructures using floating cranes and barges in waves is performed. The safety analysis consists of three components. First, the dynamic responses of the offshore structure, cranes, and barge, all of which are moored and connected using wire ropes, are analyzed. Second, tensions in the wire ropes connecting the cranes and the offshore structures are calculated. Finally, any collision between the offshore structure and the cranes or the barge that transports the offshore structure is detected. Equations of motion of the offshore structure, cranes, and barge are formulated based on multibody dynamics, as well as considering the hydrostatic, hydrodynamic, and mooring forces. Additionally, proportional-derivative control of the tagline between the cranes and the offshore structure is performed to verify the safety of the installation process, as well as for reducing the dynamic response and collisions among them.

Keywords: Marine operation, Safety analysis, Offshore structure installation, Proportional-derivative control, Multibody dynamics

1. Introduction

1.1 Background

Recently, as oceanic energy is increasingly being harnessed, many offshore structures such as wind turbines, drilling units, plants, and subsea equipment are being installed and operated at sea, as shown in Fig. 1. The installation of such offshore structures warrants the use of floating cranes, barges, or specialized vessels. Given that the operational characteristics of various installation vessels are different, the installation process is analyzed in detail. In addition, there are many additional dangers associated with offshore installation as compared with installation on land because of ocean environmental loads such as waves, currents, and winds. Thus, the dynamic responses of the offshore structure and installation vessels, as well as collisions among them should be analyzed, to ensure that the installation process is safe. If safety cannot be ensured, alternatives should be suggested, i.e., changes to the installation process. In this paper, a simulation strategy based on multibody dynamics for the installation of offshore structures is studied for analyzing installation process' safety.

[*]Corresponding author. Tel.: +82-61-450-2735, Fax.: +61-452-7774,
E-mail address: solha@mokpo.ac.kr

Fig. 1. Floating crane used for installing offshore structures

1.2 Related Works

Cha et al. (2010b) have studied the combined discrete event and discrete time simulation kernel. They developed a lifting and erection simulation framework using floating cranes in a shipyard, and integrated the open-source modules in the framework.

Cha et al. (2010c) and Ku et al. (2011) formulated equations of motion for a floating crane and a heavy cargo load based on multibody dynamics. Park et al. (2011) derived the equations of motion for a floating offshore wind turbine with an elastic tower based on flexible multibody dynamics.

Lee et al. (2010) studied the hydrostatic and hydrodynamic forces acting on a floating crane and analyzed the tension in the wire ropes between the crane and a heavy cargo load (Cha et al., 2012a). In addition, a stable numerical integration method was devised for the stiff problem of the wire ropes (Cha et al., 2010a).

In this study, we simulate the installation of an offshore structure and perform safety analysis based on the abovementioned related works. Furthermore, we propose use of the tagline proportional-derivative (PD) control method for suppressing the offshore structure's swinging motion.

1.3 Installation Scenario

In this study, we consider the use of a floating crane and a barge for installing a box-shaped offshore structure. Initially, the offshore structure is loaded on the barge and connected to the floating crane using wire ropes, as shown in Fig. 2. First, the floating crane is used to hoist up the offshore structure from the barge deck by winding the wire ropes between the booms of the floating crane and the offshore structure (Fig. 3-a). Second, the backstays and booms of the floating crane are rotated to set the offshore structure at the target position (Fig. 3-b and c). As the booms rotate, the wire ropes between the booms and the backstays unwind. Finally, the floating crane hoists down the offshore structure by unwinding the wire ropes between the booms and the offshore structure (Fig. 3-d). The hoisting and boom-rotation speeds are variables in the safety analysis described herein. The wave used here has amplitude of 1 m and frequency of 0.628/s, and is oriented at 45°.

1.4 Safety Analysis Procedure

A schematic of the safety analysis procedure used in this study is shown in Fig. 4. First of all, properties of the floating crane, barge, and offshore structures, such as mass, center of mass, mass moment of inertia, and positions of the characteristic points, are input into the equations of motion based on multibody dynamics. External forces such as hydrostatic, hydrodynamic, wire rope, mooring, and gravitational are considered in the equations

of motion. In addition, tagline control force, which maintains the offshore structure' position, is considered. After accelerations of the bodies are obtained by solving the equations of motion, their positions and velocities are calculated using the numerical integration and are visualized. We use the Hilber-Hughes-Taylor implicit integration method (Hilber et al., 1977) for ensuring numerical stability of some stiff problems. Collision detection is performed based on the shapes and positions. The simulation time is advanced and the positions, velocities, and collision positions are input into the equations of motion, external force, and control force. The equations of motion, external force, and control force are explained in subsequent chapters.

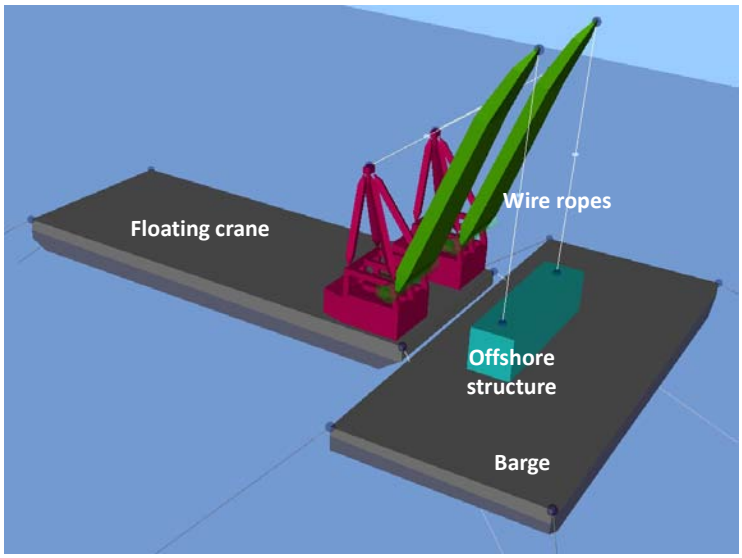

Fig. 2. Initial state of offshore structure installation in this study

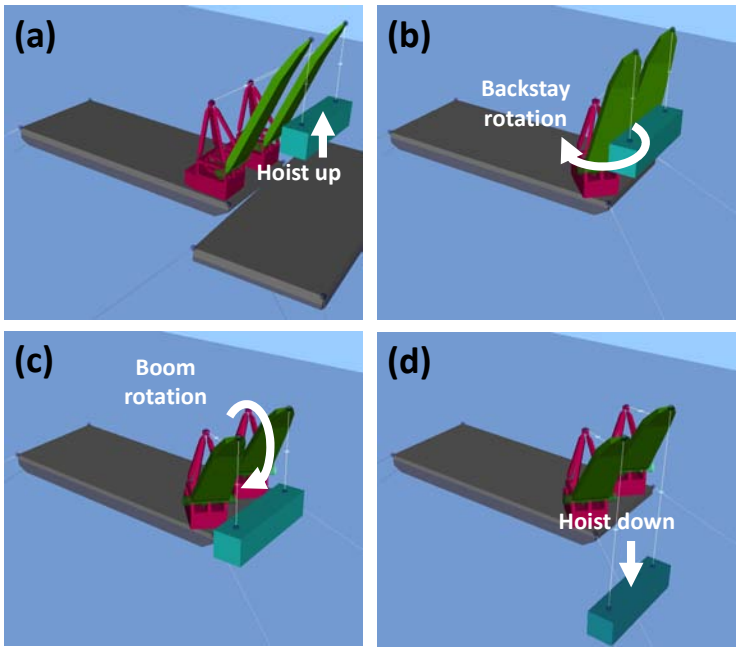

Fig. 3. Scenario for the installation of a box-shaped offshore structure: (a) hoist up the structure, (b) rotate the backstays, (c) rotate the booms, and (d) hoist down the structure

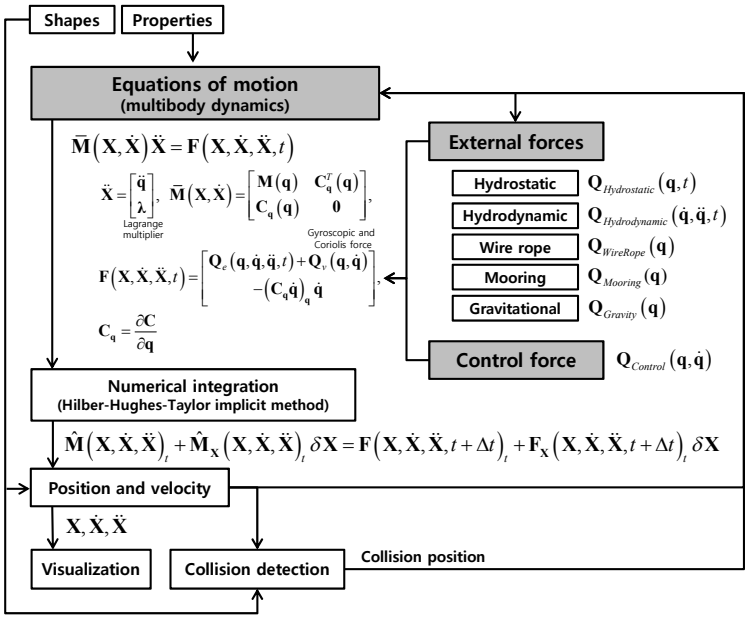

Fig. 4. Safety analysis procedure

2. Equations of Motion Based on Multibody System Dynamics

2.1 Multibody System for Offshore Structure Installation

A system in which many rigid bodies are connected physically through joints is called a multibody system (Shabana, 1994; Shabana, 2005). As shown in Fig. 5, two booms, two backstays, and the floating crane's platform form a multibody system connected through revolute joints. The principle specifications of the floating cranes and the offshore structures is noted on Table 1. In the multibody system, constraint forces acting on the bodies restrict the bodies' motion to the axial rotation. Central to multibody system dynamics is the simplification of the constraint forces among multiple bodies and the setting up of a fully coupled equation of motion.

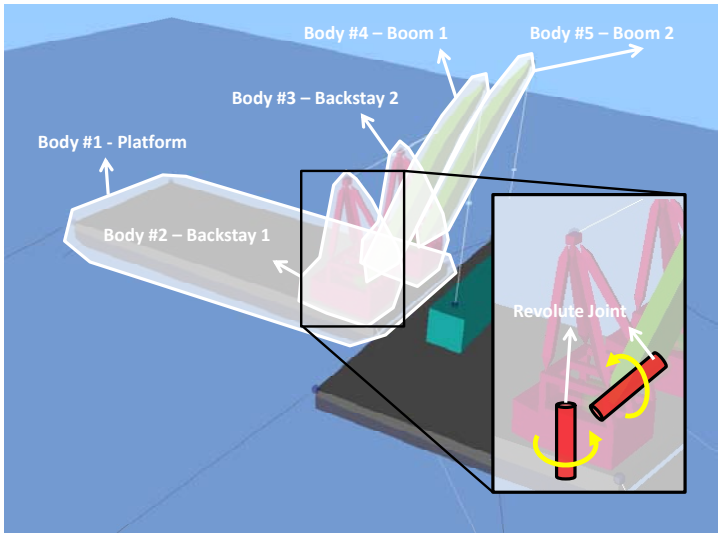

Fig. 5. Multibody system for offshore structure installation

Table 1. Specification of structures and ocean environment for offshore structure installation

Floating Crane		Offshore Structure		Ocean Environment	
Length	110 m	Length	10 m	Wave Height	0.4 m
Breadth	46 m	Breadth	40 m	Wave Frequency	0.571 rad/s
Depth	7.5 m	Height	10 m	Wave Heading Angle	45 deg
Draft	4 m	Mass	1,000 ton		
Displacement	20,746 ton				

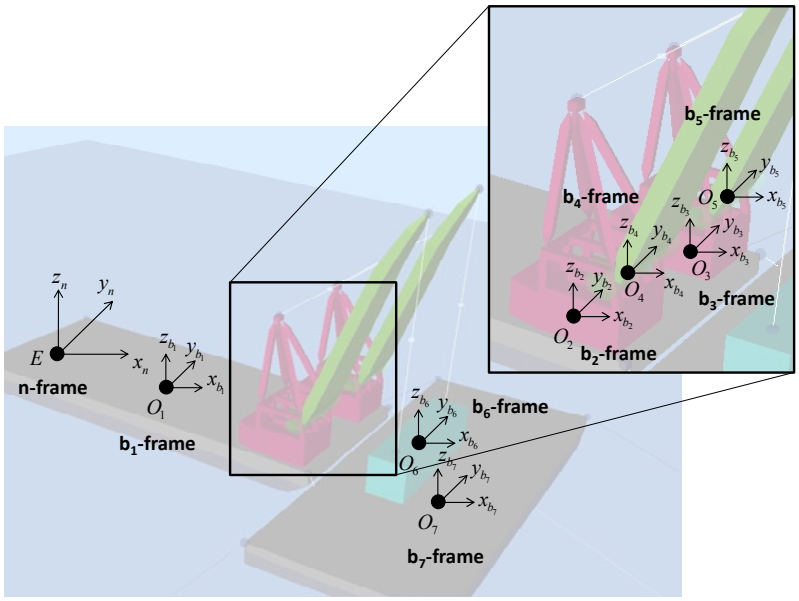

Fig. 6. Reference frames for offshore structure installation

2.2 Equations of Motion

The inertial reference frame (n-frame) and the body-fixed reference frames (b-frames) are defined, as shown in Fig. 6. The generalized coordinates consist of the position vectors of the bodies' origins and the ZYX Euler angles of the b-frames, both with respect to the n-frame.

Constraints on the revolute joints are expressed as follows:

$$C = \begin{bmatrix} C_1 & C_2 & C_3 & C_4 \end{bmatrix}^T \tag{1}$$

where C1 and C2 are the constraints between the platform and backstays 1 and 2, respectively; and C3 and C4 are the constraints between each backstay and each boom, respectively. For example, C3 is expressed as follows:

$$C_3 = \begin{bmatrix} \left[r_{O_2/E} + {}^{n}R_{b_2}\, r_{O_4/O_2} - r_{O_4/E} \right]_{(3\times1)} \\ \left[{}^{n}R_{b_4}\, y_{b_4} \bullet {}^{n}R_{b_2}\, x_{b_2} \right]_{(1\times1)} \\ \left[{}^{n}R_{b_4}\, y_{b_4} \bullet {}^{n}R_{b_2}\, z_{b_2} \right]_{(1\times1)} \end{bmatrix} \tag{2}$$

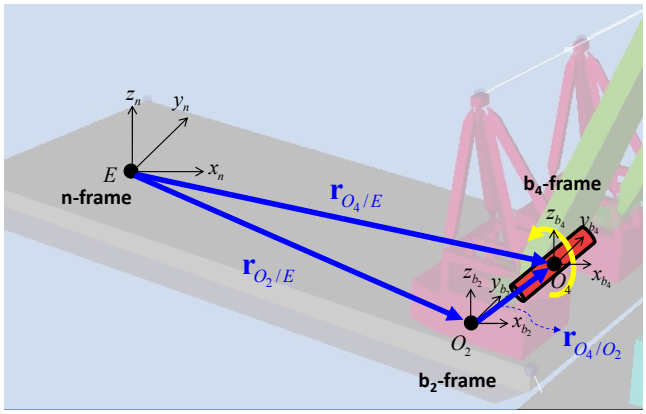

Fig. 7. Constraint between backstay 1 and boom 1

where r is position vector, R is the rotational transformation matrix between two reference frames, and x and y are the unit vectors of the axes as shown in Fig. 7.

Because the constraining forces are unknown, Lagrange multipliers are introduced to express the same. Thus, the accelerations of the multibody system and the constraining forces are calculated simultaneously from the matrix equation as follows:

$$\begin{bmatrix} M(q) & C_q^T(q) \\ C_q(q) & 0 \end{bmatrix} \begin{bmatrix} \ddot{q} \\ \lambda \end{bmatrix} = \begin{bmatrix} Q_e(q,\dot{q},\ddot{q},t) - Q_v(q,\dot{q}) \\ -\left(C_q \dot{q}\right)_q \dot{q} \end{bmatrix} \tag{3}$$

where M denotes the mass and the mass moment of inertia, C denotes the constraint matrix, q denotes generalized coordinates, λ denotes the Lagrange multiplier matrix, Qe denotes the external forces, and Qv denotes the gyroscopic and Coriolis forces. Eq. (3) is called an augmented formulation.

3. External Forces

The hydrostatic, hydrodynamic, mooring, wire rope, and gravitational forces are considered as the external forces in this study.

$$\begin{aligned} Q_e(q,\dot{q},\ddot{q},t) = {} & Q_{Hydrostatic}(q,t) + Q_{Hydrodynamic}(\dot{q},\ddot{q},t) \\ & + Q_{Mooring}(q) + Q_{WireRope}(q) + Q_{Gravity}(q) \end{aligned} \tag{4}$$

3.1 Hydrostatic Force

Because the hydrostatic force is highly nonlinear and the most dominant among the external forces, it is calculated at each time step by integrating the pressure of all fluid particles acting on the wetted surface of the floating platform under the wave elevation profile, considering the instantaneous position of the floating platform (Lee et al., 2010; Cha et al., 2010). Using the divergence theorem, we obtain the hydrostatic force exerted on the platform as follows:

$$\begin{aligned} & Q_{Hydrostatic}(q,t) \\ & = \rho g [0\ ;0\ ; \int_{Vs(q_P,t)} dV\ ; \int_{Vs(q_P,t)} y_{buoyancy} dV\ ; -\int_{Vs(q_P,t)} x_{buoyancy} dV\ ; 0]^T \end{aligned} \tag{5}$$

where ρ is the density of seawater; g is the gravitational acceleration; VS is the submerged volume of the platform; and $x_{buoyancy}$ and $y_{buoyancy}$ are the x and y coordinates, respectively, of the center of buoyancy.

3.2 Hydrodynamic Force

The hydrodynamic force acting on the platform is calculated using the three-dimensional (3D) Rankine panel method in the time domain (Kring, 1994). The velocity potential is divided into the incident potential ϕ_I and the disturbed potential ϕ_d without forward speed. The velocity potential can be calculated by solving the Laplace equation, as shown in Eq. 6.

$$\nabla^2\phi = 0, \quad \phi = \phi_I + \phi_d \tag{6}$$

The incident potential is substituted for the Froude–Krylov force, which is included in the nonlinear effect of the hydrostatic force along with the wave elevation profile. Therefore, only disturbed potential is calculated by solving the Laplace equation considering free surface and body boundary conditions.

$$\frac{\partial \eta_d}{\partial t} - \frac{\partial \phi_d}{\partial z} = 0, \frac{\partial \phi_d}{\partial t} + g\eta_d = 0 \ \ at\, z = 0 \tag{7}$$

$$\frac{\partial \phi_d}{\partial n} = \frac{\partial \delta}{\partial t} n - \frac{\partial \phi_I}{\partial n}, \delta = \xi_T + \xi_R \times x \tag{8}$$

where η_d denotes the disturbed wave amplitude; n and x denote the normal and position vectors, respectively, of the platform's wetted surface; and ξ_T and ξ_R denote the translational position and rotational angles, respectively, with respect to the b-frame. The radiation condition is regarded as Eq. 9 numerically.

$$\frac{\partial \eta_d}{\partial t} = \frac{\partial \phi_d}{\partial z} - 2\nu\eta_d + \frac{\nu^2}{g}\phi_d \tag{9}$$

where ν is the coefficient of the radiation condition. For calculating the disturbed potential, Green's second identity is used with the 3D Rankine source. For ensuring numerical stability of platform motion, an infinite-frequency added mass $M(\infty)$ should be included in the mass matrix of the floating platform and the hydrodynamic force, respectively. The hydrodynamic force is calculated using the disturbed potential and infinite-frequency added mass as follows:

$$\begin{aligned} &Q_{Hydrodynamic}(\dot{q}, \ddot{q}, t) \\ &= \left[-\iint_S \frac{\partial \phi_d}{\partial t} n dS_{(1\times 3)}; -\iint_S \frac{\partial \phi_d}{\partial t}(x \times n) dS_{(1\times 3)}; 0 \right]^T + M(\infty)\ddot{q} \end{aligned} \tag{10}$$

where S is the wetted surface of the platform.

3.3 Mooring Force

The mooring force and moment exerted on the platform are calculated using the formula given in Eq. 11 (Faltinsen, 1990).

$$Q_{Mooring}(q)=\left[\sum_{k=1}^{n}T_{H,k}(q)\cos\psi_k;\ \sum_{k=1}^{n}T_{H,k}(q)\sin\psi_k;0;\right.$$
$$\left.0;0;\ \sum_{k=1}^{n}T_{H,k}(q)\left[x_k\sin\psi_k-y_k\cos\psi_k\right]\right]^T \tag{11}$$

where TH,k and ψ_k are the force components in the horizontal direction and the angle of the k-th mooring line, respectively.

4. Tagline PD Control

4.1 Tagline PD Control Method

During the operation, wave-induced motions of the floating crane and rotational motions of the booms and backstays may cause the offshore structure to be suspended by the floating crane to swing. Therefore, it is important to develop a method for suppressing this swinging motion.

In this paper, we propose a tagline control method. The tagline connects the floating crane and the offshore structure, as shown in Fig. 8. Tension in the tagline is adjusted using a winch mounted on the deck of the floating crane. The winch is a mechanical device used for winding and unwinding the tagline. To control the tension in the tagline, we adopt the PD control method in this study.

In general, proportional-integral-derivative (PID) control can control the object more precisely than PD control. The integral control used to overcome the limits of proportional control that do not reach the target value. However, since the wire rope connected between the boom and the offshore structure was controlled to a degree of zero, it was controlled well without using the integral control.

4.2 Control Force in Equations of Motion

Fig. 9 shows the connected points of the tagline. The tagline can pull the offshore structure but does not have the capability to push it away from the floating crane. Therefore, the state of the offshore structure is classified into three cases, as shown in Fig. 9. The PD control method is then applied to each case.

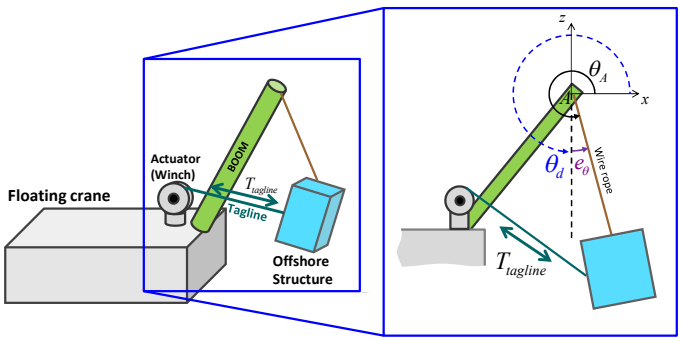

Fig. 8. Tagline control method proposed in this paper

- Case A: $f\left(\dot{\theta}_A \geq 0 \text{ and } e_\theta \geq 0\right)\left\{T_{tagline}=K_p\cdot e_\theta+K_d\cdot\dot{e}_\theta\right\}$ (12)

- Case B: $f\left(\dot{\theta}_A \geq 0 \text{ and } e_\theta < 0\right)\left\{T_{tagline}=K_d\cdot\dot{e}_\theta\right\}$ (13)

- Case C: $if\ \left(\dot{\theta}_{l/A}<0\right)\left\{T_{tagline}=0\right\}$ (14)

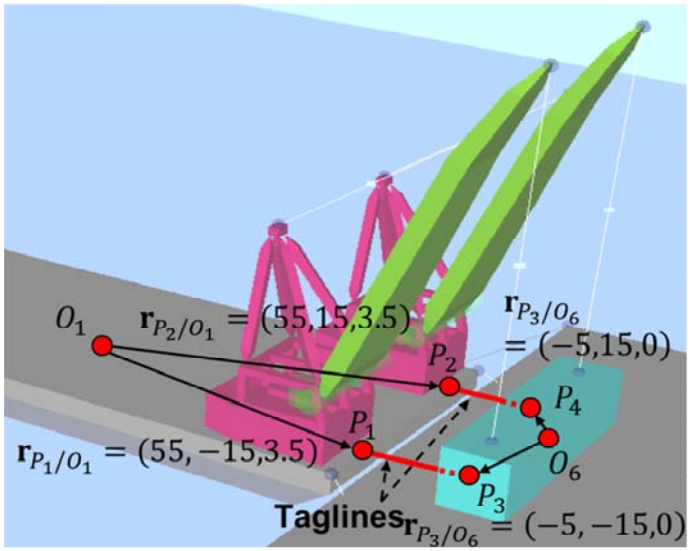

Fig. 9. Connected points of tagline

where K_p and K_d are user-defined values of the proportional and derivative gains, respectively. Thus, the control force is expressed as follows:

$$Q_{Control}(q,\dot{q}) = T_{tagline}\, u_{tagline} \tag{15}$$

where $u_{tagline}$ is the unit vector of the connecting point on the floating crane with respect to the connecting point on the offshore structure.

5. Safety Analysis of Offshore Installation

5.1 Dynamic Response of Offshore Structure

Fig. 11 shows the surge motion of the offshore structure, whose initial position is 74.0 m. The minimum surge motion is 66.0 m when the backstays are rotated and the booms are almost upright, and the maximum value is 81.8 m when the offshore structure is hoisted down. Because the offshore structure moves with amplitude of 7.1 m at that time, it may be off the target position by within 3 m in the surge direction.

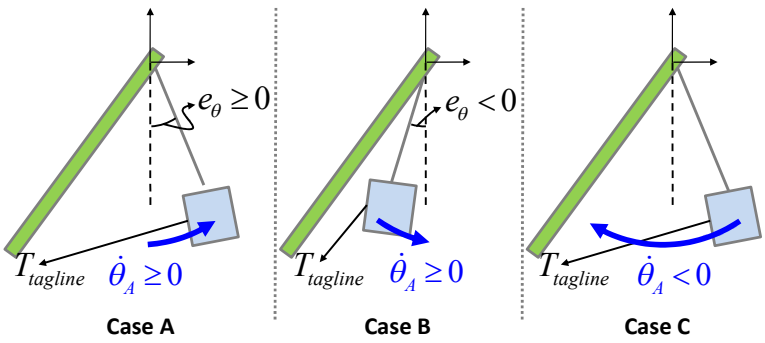

Fig. 10. Three cases of offshore structure for tagline PD control

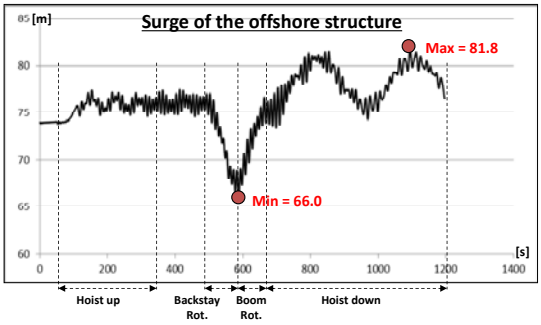

Fig. 11. Dynamic response: surge of offshore structure

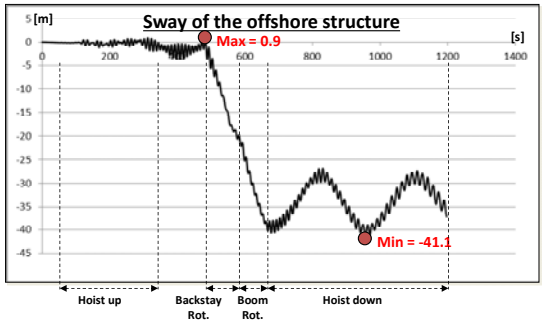

Fig. 12. Dynamic response: sway of offshore structure

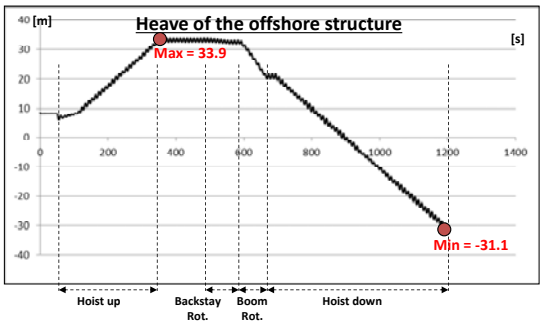

Fig. 13. Dynamic response: heave of offshore structure

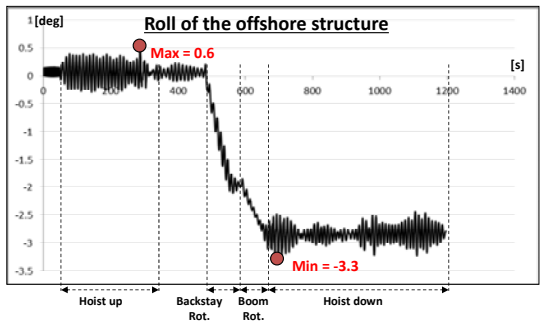

Fig. 14. Dynamic response: roll of offshore structure

The sway motion of the offshore structure is shown in Fig. 12. While the backstays and the booms rotate, the offshore structure moves to the negative position in the surge direction. When the offshore structure is hoisted down, the amplitude of this sway motion is 14 m. Thus, the sway motion is more critical than the surge motion in this case.

Fig. 13 shows the heave motion of the offshore structure. The structure rises when it is hoisted up, and it goes down when it is hoisted down without unexpected features. In addition, the amplitude of the heave motion is very small.

The offshore structure inclines in the roll direction, as shown in Fig. 14, while the backstays and the booms are being rotated. The offshore structure moves to the starboard of the floating crane; thus, the roll motion of the floating crane affects the roll motion of the offshore structure.

The pitch motion of the offshore structure has an amplitude of 9.5 m, as shown in Fig. 15; thus, this motion is more critical than the roll motion in this case.

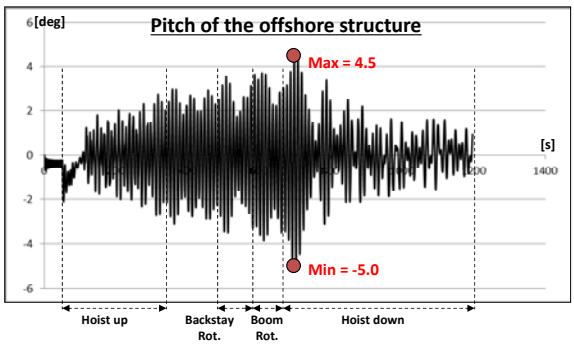

Fig. 15. Dynamic response: pitch of offshore structure

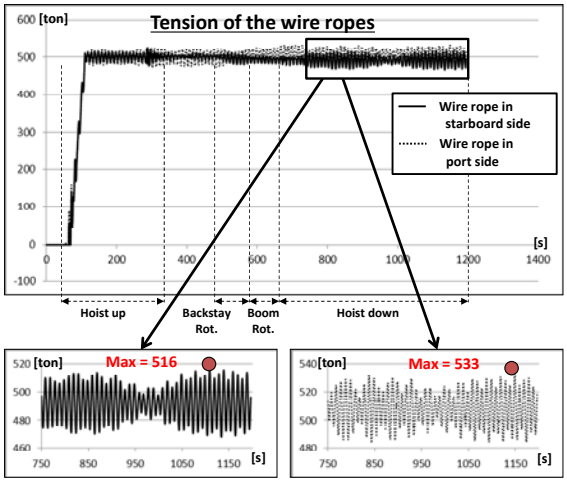

Fig. 16. Tension in the wire ropes on starboard and port sides

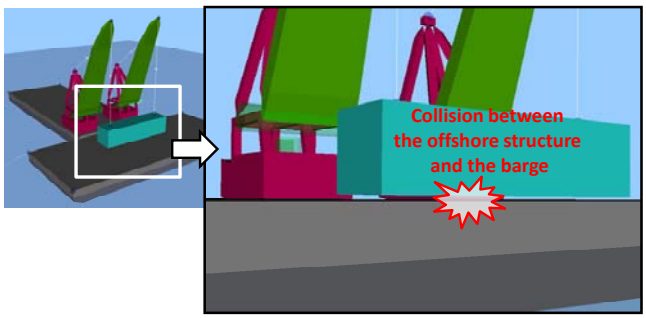

Fig. 17. Collision between offshore structure and barge

5.2 Tension in Wire Ropes between Floating Crane and Offshore Structure

Fig. 16 shows the tension in the wire ropes connecting the floating crane and the offshore structure. The solid and dotted lines represent the tension in the wire rope on the starboard and port sides, respectively. While the offshore structure heels to the starboard side, the tension in the wire rope on the starboard side is higher than that on the port side. The maximum values are 516 ton and 533 ton. The dynamic amplitude factors are 1.03 and 1.06 for a static tension of 500 ton.

5.3 Collision Detection between Offshore Structure and Barge

Collisions between the offshore structure and the barge occur when the offshore structure is about to be lifted off the barge. The barge floats up because although it loses the weight of the offshore structure, its buoyancy is the same as that in the loaded condition. Increased hoisting speeds can reduce the number of such collisions.

To check the collisions between the offshore structure and the barge, this study simply checked an interference between the bottom plane of the offshore structure and the top plane of the barge. When the interference occurred, the reaction force is calculated in the opposite direction of penetration using proper stiffness and penetrated depth, and it is reflected in the external forces of the equations.

6. Conclusions

In this study, we carried out a safety analysis of the process of installing an offshore structure using a floating crane and a barge. The results of a dynamic response analysis show that the offshore structure could be

off the target installation position within 3 m in the surge direction and 7 m off in the sway direction. Rotation of the backstays increases the sway motion. In addition, the pitch motion is more critical than the roll motion because two wire ropes are connected to the starboard and port sides. The dynamic amplitude factors of the wire ropes between the floating crane and the offshore structure are 1.03 and 1.06 with respect to the static tensions. A fast hoisting speed can reduce the number of collisions between the offshore structure and the barge when the offshore structure is lifted off the barge.

In future, various dynamic factors based on different ocean environment and operational conditions will be analyzed. Furthermore, the results of such analysis will be validated.

Acknowledgements

This works was supported by (a) the project “Development of Core Installation Technologies for Float-over and Dual Crane Methods”, which is supported by the Ministry of Oceans and Fisheries, and (b) Mokpo National University SURF R&D Center Infrastructure Project(Project ID : N001079).

References

Cha, JH, Ku, NK, Roh, MI, and Lee, KY, *Dynamic Simulation of a Shipbuilding Erection Crane based on Wire Rope Dynamics*, Journal of Computational Structural Engineering Institute of Korea, 25 (2) (2012a) 119-128 (Korean).

Cha, JH, Park, KP, and Lee, KY, *Development of a Simulation Framework and Applications to New Production Processes in Shipyards,* Computer-Aided Design, 44 (3) (2012b) 241-252.

Cha, JH, Park, KP, and Lee, KY, *Numerical Analysis for Nonlinear Static and Dynamic Response of a Floating Crane with Elastic Boom,* Trans. of the KSME(A), 34 (4) (2010a) 501-509 (Korean).

Cha JH, and Roh, MI, *Combined Discrete Event and Discrete Time Simulation Framework and Its Application to the Block Erection Process in Shipbuilding,* Advances In Engineering Software, 41 (4) (2010b) 656-665.

Cha, JH, Roh, MI, and Lee, KY, *Dynamic Response Simulation of a Heavy Cargo Suspended by a Floating Crane Based on Multibody System Dynamics*, Ocean Engineering, 37 (14-15) (2010c) 1273-1291.

Faltinsen, OM, *Sea Loads on Ships and Offshore Structures*, University of Cambridge (1990).

Hilber, HM, Hughes, TJR, and Taylor, RL, *Improved Numerical Dissipation for Time Integration Algorithms in Structural Dynamics*, Earthquake Engineering and Structural Dynamics, 5 (1977) 283-292.

Kring, DC, *Time Domain Ship Motions by a Three-Dimensional Rankine Panel Method*, MIT, Ph.D Thesis (1994).

Ku, NK, Jo AR, Ha, S, Friebe, M, Cha, JH, Park, KP, and Lee, KY, Development of a Multibody Dynamics Kernel for Motion Analysis of a Floating Wind Turbine, *Proceedings of the 21st ISOPE(International Offshore and Polar Engineering Conference) 2011*, Maui, Hawaii, USA, 383-390 (2011).

Lee, KY, Cha, JH, and Park, KP, *Dynamic Response of a Floating Crane in Waves by Considering the Nonlinear Effect of Hydrostatic Force*, Ship Technology Research, 57 (1) (2010) 62-71.

Park, KP, Cha, JH, and Lee, KY, *Dynamic Factor Analysis for the Heavy Lifting Operation Considering an Elastic Boom Effects*, Ocean Engineering, 38 (10) (2011) 1100-1113.

Shabana, AA, *Computational Dynamics*, John Wiley & Sons, INC (1994).

Shabana, AA, *Dynamics of Multibody Systems*, 3rd edition, Cambridge University Press (2005).